ISSN 1648-7788 / eISSN 1822-4180

VILNIUS TECH
Vilnius Gediminas Technical University

AVIATION

2024
Volume 28
Issue 4
Pages 279–291
https://doi.org/10.3846/aviation.2024.22718

ENHANCING UAS SAFETY THROUGH BUILDING-INDUCED DANGEROUS ZONES PREDICTION: CONCEPT AND SIMULATIONS

Renata BALAZOVA [1]✉, Jiri HLINKA [1], Petr GABRLIK [2,3], Alessandro SANTUS [4], Simone FERRARI [4]

[1]*Institute of Aerospace Engineering, Faculty of Mechanical Engineering, Brno University of Technology, Technicka 2896/2, 61669 Brno, Czech Republic*
[2]*Faculty of Electrical Engineering and Communication, Brno University of Technology, Technicka 3058/10, 616 00 Brno, Czech Republic*
[3]*Central European Institute of Technology, Brno University of Technology, Purkynova 656/123, 612 00 Brno, Czech Republic*
[4]*Department of Civil, Environmental Engineering and Architecture, University of Cagliari, via Marengo 2, 09123 Cagliari, Italy*

Article History:
- received 19 July 2024
- accepted 22 October 2024

Abstract. This study presents a comprehensive approach to operational estimation of the zones of danger for the Unmanned Aerial Systems (UASs) generated at low altitudes in presence of buildings, aimed at ensuring their safer operation. The main tasks are three. The first one is the definition of an inboard measurement methodology appropriate and feasible for UAS that allows Eddy Dissipation Rate (EDR) estimation. An inboard setup with a lightweight and low-cost anemometer operating at a 1 Hz sampling rate, immediately usable on UAS, is proposed. The second one is the definition of empirical equations to estimate the size of dangerous areas for the UAS flights around buildings through numerical simulation. The third one is the validation of the empirical formulas in a real-world case, through the numerical simulation of a group of buildings belonging to a research centre. Results show a good resemblance in the size of the danger zones, highlighting that this multi-faceted approach contributes to enhanced safety protocols for UASs operating in urban environments.

Keywords: Eddy Dissipation Rate, sonic anemometer, UAS, numerical simulation, real-time data, building induced danger zones.

✉Corresponding author. E-mail: *renata.balazova@vut.cz*

1. Introduction

The rapid proliferation of Unmanned Aerial Systems (UAS) in civilian airspace presents both unprecedented opportunities and significant challenges (Yuan et al., 2024).

While UASs promise to revolutionize industries from logistics and agriculture to infrastructure inspection, their safe integration into complex environments, particularly in proximity to buildings, demands careful consideration of aerodynamic factors. Turbulence, with its unpredictable gusts and eddies, poses a particular threat to UASs, especially to smaller multirotor platforms. These disturbances lead to loss of control, instability, and potentially catastrophic collisions, jeopardizing not only the UAS itself but also people and property on the ground.

Despite the growing recognition of this risk, existing aviation meteorological information often lacks accurate, real-time turbulence data for low-altitude operations near buildings. This gap, highlighted by previous research (Balážová et al., 2024) and numerous anecdotal reports from UAS operators, underscores the urgent need for reliable and cost-effective turbulence detection solutions.

Prior research on drone-based wind measurement (e.g., Palomaki et al., 2017; Adkins, 2019) has established ultrasonic anemometers as the ideal technology for capturing three-dimensional wind data. However, existing research has primarily focused on high-cost, high-frequency anemometers, which are often impractical for smaller UAS platforms due to weight and budget constraints (Adkins, 2019). High-quality ultrasonic anemometers range in cost from €1,500 to €20,000 and weigh between 0.225 kg and 2.150 kg, making them unsuitable for many smaller UASs.

This study builds upon prior work (Balážová et al., 2024), which identified the Eddy Dissipation Rate (EDR) as a key metric for turbulence assessment and explored the potential of using affordable sonic anemometers for real-time data collection (International Civil Aviation Organization [ICAO], 2001). However, the standard EDR algorithm,

designed for commercial aircraft with high-frequency sensors, requires adaptation for use with UAS platforms that typically have lower sampling rates (1 Hz).

This approach is distinguished by its focus on developing a turbulence estimation system specifically designed for the limitations of low-cost, low-frequency sensors found on smaller UAS platforms.

While previous studies like Galway et al. (2011) focused on modelling urban wind field effects on UAS flight using high-fidelity simulations and data from specialized sensors, this research aims to provide a more practical and accessible solution for smaller UAS operators. So, the first task of this paper is to identify and test a low-cost, low-weight sensor to measure the wind velocity on board an UAS, and then to validate its measurements through a comparison between in-field measurements, performed under real-world conditions, and laboratory measurements, performed under controlled and repeatable conditions.

On the other hand, the number of UAV flights in the urban environments has rapidly increased during the last years, for instance for the delivery of goods (Ezaki et al., 2024), or to deliver automated defibrillators in cases of cardiac arrest (Kristiansson et al., 2024).

This has raised the attention of the scientific communities and companies on the integration of UAVs and urban built environments (Chrit, 2023).

When the wind interacts with a building, the flow detachment phenomenon arises, creating dangerous vortices and wakes that can results in difficulties for the UAV flights and manoeuvres, due to the fast changes in air direction and magnitude (see, among the others, Chrit & Majdi, 2022, and Galway et al., 2012).

Consequently, various investigations have been devoted to deepening the knowledge on that interaction, employing both numerical and laboratory techniques. For instance, Pensado et al. (2024) have performed numerical simulations on a model of a typical city centre, already employed as an example in other numerical studies, including buildings of various heights and shapes, focusing on the turbulence development in the whole model and on an external path for the UAV to go from a starting to an arrival point, both external to the city model.

Diop et al. (2022) have numerically studied a single high-rise building, but their focus was on identifying the optimal position for pressure sensors to reconstruct the wind wake features of a characteristic wind, but without varying the building dimensions and the wind velocity.

Regarding the laboratory experiments, Frey et al. (2024) have studied in the wind tunnel the effect of a built environment, representative of a typical European city downtown, with the target to plan the UAV flights, while Yuan et al., 2024) focused, in their water tunnel experiments on the velocity field around a single wing moving near a single building of a simplified shape.

Investigations on site-specific or complex building arrangements provide useful information on the particular configuration but are difficult to generalize. Moreover, a parametric investigation on the relation between the flow detachment zones, potentially dangerous for the UAV flights, the building dimensions and the wind velocity is, to the best authors' knowledge, missing. For this reason, the second task of this paper is to investigate the size of the dangerous zones for the UAV manoeuvres, when the size of a single building and the wind velocity are systematically varied, proposing some empirical formulas for predicting the extent of hazardous zones, such as downstream wake areas and building edge updrafts, that can be used to evaluate them.

To achieve this target, numerical simulations using the Envi-met software were performed, a holistic three-dimensional non-hydrostatic model designed by Bruse and Fleer (1998) for simulating surface-plant-air interactions. In recent years, ENVI-met has been widely applied in the field of urban wind environment (Szucs, 2013; Wang & Lv, 2019; Chiri et al., 2020), mainly to evaluate the microclimate performances of existing or planned built environments.

Eventually, the third task of this paper is to perform a preliminary validation of the proposed formulas, arising from the single building simulations, on a more complex real-world built environment. For this scope, the AdMaS Centre at Brno University of Technology (Brno, Czech Republic) has been numerically simulated and the size of the dangerous zones for the UAV flights around a building compared with the ones calculated with the proposed formulas.

The rest of this paper is organized as follows. Section 2 is devoted to identifying, select and test a low-cost sonic low-weight anemometer suitable for UAS integration. In Section 3, the dimensions of the dangerous zones for the UAV flights around a single building are studied through numerical simulations and two formulas for this scope are proposed. Section 4 shows the numerical simulations on the AdMaS Centre case and the comparison between the results from this simulation and the above quoted formulas is discussed. Eventually, the conclusions are drawn in Section 5.

2. Materials and methods selection and validation

2.1. Sensor selection

The selection of the Calypso "Ultrasonic Portable Mini" anemometer with a 1 Hz sampling rate was guided by several key considerations, primarily the need to balance measurement accuracy with the practical constraints of UAS integration. High-frequency anemometers, while offering more detailed turbulence data, often come with significant cost and weight penalties, as highlighted by Adkins (2019). These factors can be prohibitive for smaller UAS platforms with limited payload capacity. The Calypso anemometer, with its compact size (0.078 kg) and affordability, aligns with the recommendations of Patrikar et al.

(2020) for utilizing low-cost, lightweight sensors in UAS applications. This choice allows for broader accessibility and feasibility for researchers and operators working with smaller UAS, promoting wider adoption of turbulence estimation capabilities.

While the 1 Hz sampling rate is lower than that used in some studies focusing on high-resolution turbulence characterization, it is crucial to consider the specific context of this research. This study focuses on characterizing turbulence in the vicinity of buildings, where the turbulent eddies are typically larger and evolve more slowly compared to those encountered at higher altitudes or in the free atmosphere. Therefore, a 1 Hz sampling rate is deemed sufficient to capture the dominant turbulence scales relevant to UAS operations in this specific environment. This aligns with the principle of selecting sensors and sampling rates that are appropriate for the specific phenomena being investigated.

To mitigate the potential limitations of the lower sampling rate, rigorous validation of the sensor's accuracy was performed. This involved wind tunnel testing under controlled conditions, as detailed in the subsequent section. The validation process confirmed the sensor's ability to provide reliable wind measurements within the range of wind speeds relevant to UAS operations near buildings. This validation process ensures that the chosen sensor, despite its lower sampling rate, provides accurate and reliable data for the specific application of this research.

The choice of a 1 Hz anemometer also aligns with the broader objective of this research, which is to develop a practical and accessible turbulence estimation system for smaller UAS platforms. By utilizing a readily available, cost-effective sensor, this research aims to provide a solution that can be easily adopted by a wider range of users, thereby contributing to enhanced safety and operational efficiency in UAS applications. This focus on practicality and accessibility promotes the broader impact of the research and its potential to improve UAS operations in real-world scenarios.

In summary, the selection of the Calypso anemometer with a 1 Hz sampling rate was a carefully considered decision that balanced the need for accurate turbulence characterization with the practical constraints of UAS integration. The rigorous validation process and the focus on relevant turbulence scales ensure the reliability and applicability of the chosen sensor for this research.

2.2. Sensor validation

Therefore, prior to UAS integration, the Calypso anemometer underwent wind tunnel testing (Figure 1) to assess its accuracy under controlled conditions. The anemometer was tested across a range of wind speeds from 1 m/s to 15 m/s (Figure 2), with each velocity maintained for 60 seconds. This testing methodology, like that employed in Giersch et al. (2022), allows for systematic evaluation of the sensor's performance. The tested wind speeds (1 m/s to 15 m/s) are those most relevant to UAS operation, including gusty conditions near buildings (Mohamed et al., 2023).

Furthermore, this approach diverges from previous work that relied on high-frequency sensors and comprehensive flight data typically available on commercial aircraft (NCAR). Instead, the Eddy Dissipation Rate (EDR) calculation methodology to accommodate the lower sampling rate (1 Hz) and limited sensor suite of the UAS platform were adapted. This adaptation enables to estimate turbulence in real-world conditions. It bridges the gap between theoretical models and practical applications for smaller UAS operators.

As shown in Table 1, the observed deviations exceeding 10% at wind speeds below 3 m/s are not unexpected. Such deviations are common in aerodynamic measurements at low speeds, often attributable to the limitations of both the reference and testing sensors. While the Calypso sonic anemometer is specified for accurate measurements at wind speeds of 1 m/s and above, the Venturi tube, used as a reference device, may not be ideally suited for precise measurements at very low flow velocities. Therefore, it's likely that both the Venturi tube and the Calypso anemometer contribute to the observed deviations at wind speeds below 3 m/s. However, for wind speeds above 3 m/s, the Calypso anemometer demonstrated high precision, consistently exhibiting deviations below 10% (and below 3% for wind speeds above 7 m/s). It's important to note that low wind velocities generally pose a lesser risk to UAS flights compared to increased wind speeds.

Figure 1. Calypso sonic anemometer located in the wind tunnel during verification tests

Table 1. Results of the sonic anemometer accuracy verification tests, using a wind tunnel venturi tube as reference

Level	Calypso data 60 sec average [m/s]	Wind tunnel data 60 sec average [m/s]	Deviation 60 s Average [m/s]	% deviation
1	0.530	0.227	0.447	84.35
2	1.755	1.238	0.783	44.63
3	3.067	2.772	0.388	12.66
4	4.392	4.174	0.324	7.38
5	5.690	5.552	0.230	4.04
6	6.968	6.838	0.228	3.28
7	8.242	8.159	0.181	2.19
8	9.568	9.476	0.208	2.18
9	10.897	10.818	0.168	1.54
10	12.233	12.149	0.175	1.43
11	13.595	13.491	0.171	1.26
12	14.998	14.839	0.241	1.61
13	16.387	16.211	0.218	1.33
14	17.918	17.575	0.397	2.21
15	19.351	18.957	0.445	2.30

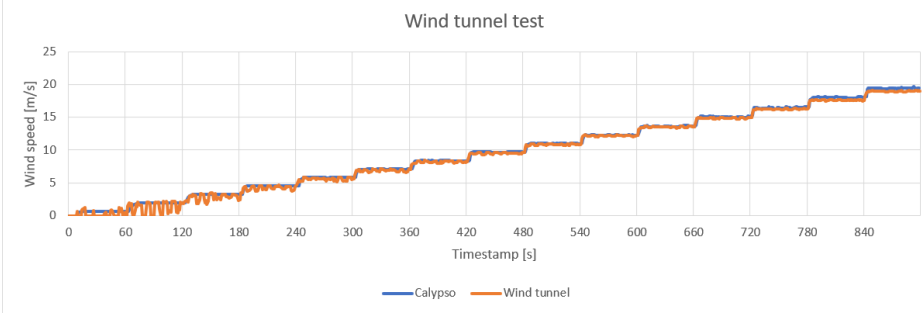

Figure 2. Dependency between time (horizontal axis) and wind speed (vertical axis) clearly shows low measurement precision below 3 m/s, but sufficient precision above

2.3. UAS integration and flight tests

Following wind tunnel validation, the Calypso anemometers were integrated onto the DJI M100 four-rotor UAS (Figures 3) fitted with the Cube Orange+ autopilot module running the PX4 flight stack. The Calypso devices were mounted on a custom-built carbon tube, 148 cm apart. This distance ensured sufficient clearance from the rotors to avoid influencing the measurements (Adkins et al., 2020). Initial flight tests focused on assessing the UAS's manoeuvrability and stability with the added sensors, as well as verifying the reliability of the Bluetooth data connection and the effectiveness of the data logging process. These tests ensured the system's operational readiness for the subsequent field experiments.

To establish a reliable ground truth reference for in-situ wind measurements during UAS flight tests, a Davis Vantage Pro2 meteorological station (Figure 4) was employed. This research-grade meteorological station (Davis Vantage Pro2) records a wide range of meteorological data. This includes wind speed (up to 90 m/s), temperature, humidity, barometric pressure, and rainfall.

The Vantage Pro2 served as a ground-based reference to validate wind speed measurements acquired by the onboard Calypso anemometer during a dedicated test flight. The UAS was operated at an approximate altitude of 2 meters above the terrain, corresponding to the elevation of the Davis anemometer. Comparison of the data from both sensors (Figure 5) revealed a high degree of agreement. This substantiates the accuracy and reliability of the wind measurements. Due to the different position of both ground- and air-based anemometers (Figure 4), small deviations observed were expected.

Furthermore, the Davis Vantage Pro2 is poised to play a pivotal role in the forthcoming demonstration mission. Precise measurements of ground-level wind speed and direction will be used to accurately calibrate the numerical simulations and assess the real-world performance of the turbulence prediction models.

a) b)

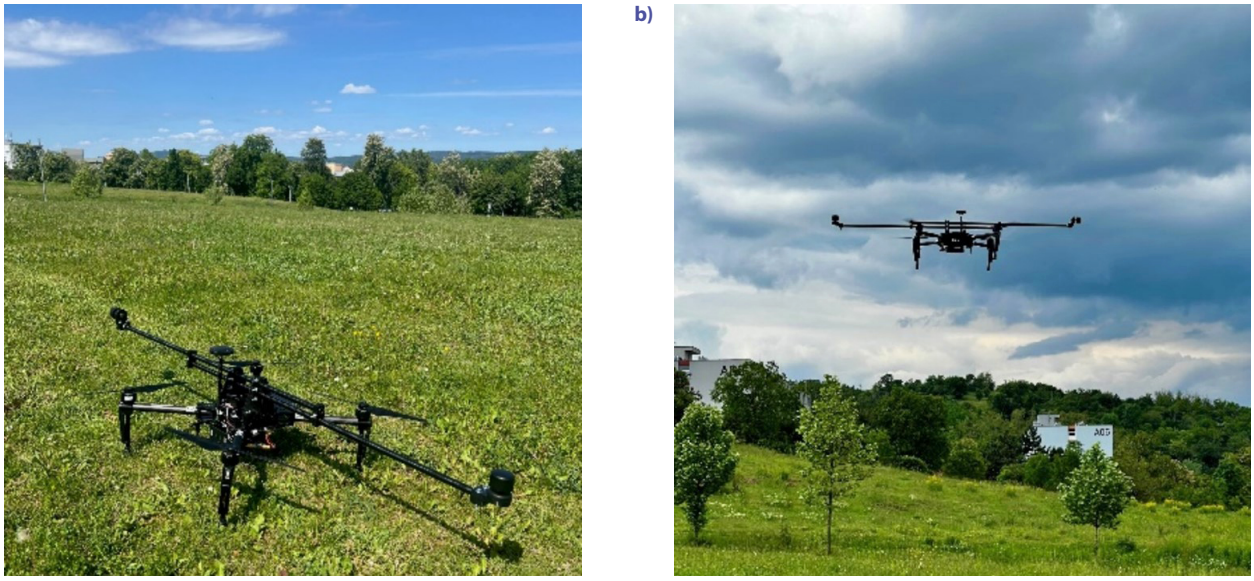

Figure 3. The DJI M100 UAS fitted with two Calypso anemometers: a – detailed view before the commencement of the flight, b – during performing the initial flight test

a) b)

Figure 4. Ground-based reference: a – meteorological station Davis Vantage Pro2 during UAS test flight, b – console displaying measured values

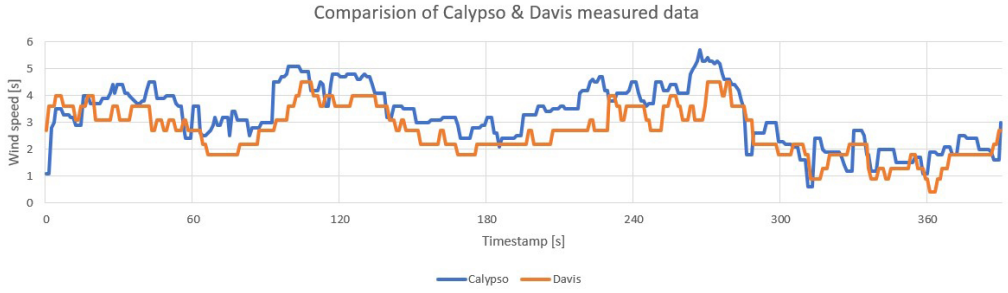

Figure 5. The comparison of the data from the ground-based reference and the anemometer onboard UAS in flight

2.4. Eddy dissipation rate calculation

The Eddy Dissipation Rate (EDR) is a key turbulence metric. The inertial dissipation method using structure function (Kim et al., 2021) was selected for EDR calculation, as detailed in previous work (Balážová et al., 2024). This method was adapted for a 1 Hz sampling rate by adjusting the range of temporal separation (τ) and extending the time window for analysis. Preliminary flight tests, including hovering manoeuvres, allowed for the measurement of baseline EDR values and further refinement of the calculation methodology.

3. Numerical simulations for the definition of the dangerous zones for the UAV flights around a single building

A series of numerical simulations were conducted to assess the impact of buildings on the development of dangerous zones for the UAV flight and inform the development of safety guidelines for UAS operations. The first scenario involved stand-alone buildings of varying heights (5 m to 20 m) under different undisturbed wind speed conditions (2 m/s to 10 m/s), with constant wind direction. The objective was to obtain quantitative information about the size of the dangerous zones for the UAV flight and to define two empirical equations to predict their size.

Numerical simulations were performed using ENVI-met, (Version 5.6.1, ENVI_MET GmbH, Essen, Germany, Bruse & Fleer, 1998) a holistic three-dimensional non-hydrostatic model designed for simulating surface-plant-air interactions. ENVI-met is based on the principles of Fluid Mechanics, Thermodynamics, and Atmospheric Physics. This allows it to calculate various parameters, including three-dimensional wind fields, turbulence, air temperature, and humidity. In particular, the spatial and temporal evolution of the wind field is calculated by applying the non-hydrostatic incompressible three-dimensional Reynolds Averaged Navier-Stokes (RANS) equation, and turbulence is parametrized using a $E - \varepsilon$ 1.5 order closure model. Based on the work of Mellor and Yamada, 1975, the $E - \varepsilon$ model basically consists of two prognostic equations, one describing the production of turbulent kinetic energy (TKE) and the other its dissipation. In contrast to first order closure models, the $E - \varepsilon$ model allows the simulation of advective processes in horizontally inhomogeneous environments without as much computation time as closure models of higher order (Simon et al., 2021).

According to Fabbri and Costanzo (2020), ENVI-met is the most widely used software for simulating the urban outdoor microclimate. ENVI-met proves to be a suitable tool for analysing wind fields in the built environment. It is especially effective when considering the interaction of wind with obstacles of different natures, such as buildings and vegetation. The ability to replicate daily variations in sun position and user-selected meteorological conditions enhances its applicability. This makes ENVI-met useful not only for microclimatic analyses but also for other objectives, such as those pursued in the present study. For instance, these features are fundamental for the simulation of the AdMas Centre (see Section 4), which involved modelling an existing area with buildings and various types of vegetation and soil, under real world conditions.

As every numerical code, ENVI-met has some inherent limitations. One limitation is related to the spatial discretization of the domain, as only cubic cells can be employed (with a minimum cell side dimension of 0.5 m) and the grid resolution (in other words, the cell size) cannot be varied along the domain, as in other numerical models. Moreover, being a RANS-based software, some approximations are introduced by the averaged numerical solution of complex equations: in fact, in RANS simulations, only the mean fields are directly computed, while the turbulent spectrum is modelled via some specific turbulence models, with the scope to estimate the effect of turbulent motions on the mean fields. In addition, the turbulence models are mostly of empirical or semi-empirical nature, typically with some coefficients or parameters which need to be finely tuned to obtain accurate results, and this introduces a certain level of uncertainty, in particular when novel or not common turbulence closures are employed. On the other side, RANS models as ENVI-met have computational costs which are dramatically smaller when compared to the other two main numerical simulation techniques of flows, like Large Eddy Simulation (LES) and Direct Numerical Simulation (DNS), making it more suitable for simulations linked to practical applications. More details on numerical simulations, as well as on their features, advantages and limitations, can be found in Ferrari et al. (2022).

3.1. Stand-alone building simulations

A comprehensive set of numerical simulations was conducted to assess the size and location of hazardous zones for Unmanned Aircraft Systems (UAS) operations in the vicinity of stand-alone buildings. The simulations examined a range of building heights, from 5 meters to 20 meters, and considered the effects of varying meteorological conditions, with undisturbed wind speeds spanning from 2 m/s to 10 m/s. The primary objective of this study was to characterize the spatial extent of dangerous areas resulting from flow detachment phenomena induced by the interaction of wind with the built environment. Specifically, the investigation focused on the two most dangerous zones around the building and characterized by a strong change in the wind flow due to the interaction with the building.

The first hazardous zone is the building's downstream wake. This region, located directly behind the building, is characterized by low wind speeds, altered flow patterns, and shifting wind directions due to wake vortices. The significantly reduced wind speed and altered wind direction in this zone pose a risk to UAS due to abrupt changes in aerodynamic forces. The second one is the vertical updraft zone, located above the building rooftop, which appear as strong upward airflows near the upstream edges of buildings that cause undesirable lift, potentially leading to loss of control or collisions.

As above stated, the ENVI-met software was employed to model the intricate dynamics between wind flow and building geometry. Multiple simulation scenarios were executed, systematically varying building height and wind speed to capture the diverse range of potential flow field configurations. The spatial domain for each simulation was carefully tailored to the specific dimensions of the building under investigation, ensuring the flow reattachment inside the domain and, consequently, a representative and accurate simulation environment (Table 2). A uniform grid cell resolution of 1 m x 1 m x 1 m was maintained across all simulations.

For each simulation, the date and time were consistently set to April 15th, 2024, at 7:00 AM, with a total simulation duration of 5 hours. Meteorological parameters were established using a simple forcing method with a 24-hour cycle and automatic linear interpolation. The minimum and maximum temperatures were set to 18° Celsius and 28° Celsius, respectively, while the minimum and maximum relative humidity values were 45% and 75%, respectively. Wind direction was consistently oriented to the North, as determined by a thorough analysis of wind rose data for the AdMaS center. Five wind speeds (2, 4, 6, 8, and 10 m/s) were selected for each building height. This resulted in a total of 20 numerical simulations, each exploring a single building scenario under varying wind conditions. Figure 6 illustrates an example of the velocity field (the colors highlight the magnitude, while the vectors both the magnitude and the direction) in a vertical section in the center of a single building, obtained as output for a 10 m x 10 m x 20 m building subjected to a 10 m/s wind, at 12:00.

The downstream wake distance is defined as the distance between the building and the point where the wind speed recovers to 25% of its initial value. This distance is measured at ground level in a vertical section of the velocity field at the building's midpoint (see Figure 6). For example, in simulations with a 10 m/s wind speed, the downstream wake zone extends from the building's downstream wall to the point where the wind speed exceeds 2.5 m/s. The measurement at ground level is needed because, for the UAS safety, also the take-off and landing need to be done in a safe zone. The downstream wake distance has been measured for each simulated case and its values are shown in Figure 7, versus the building height, for each

Table 2. Computational domain dimensions for simulated building heights and wind speeds

Building size (width, length, height) [m]	Domain size [m]	Wind speed [m/s]
10 x 10 x 5	60 x 85 x 25	2,4,6,8 and 10
10 x 10 x 10	110 x 160 x 50	2,4,6,8 and 10
10 x 10 x 15	160 x 235 x 75	2,4,6,8 and 10
10 x 10 x 20	210 x 310 x 100	2,4,6,8 and 10

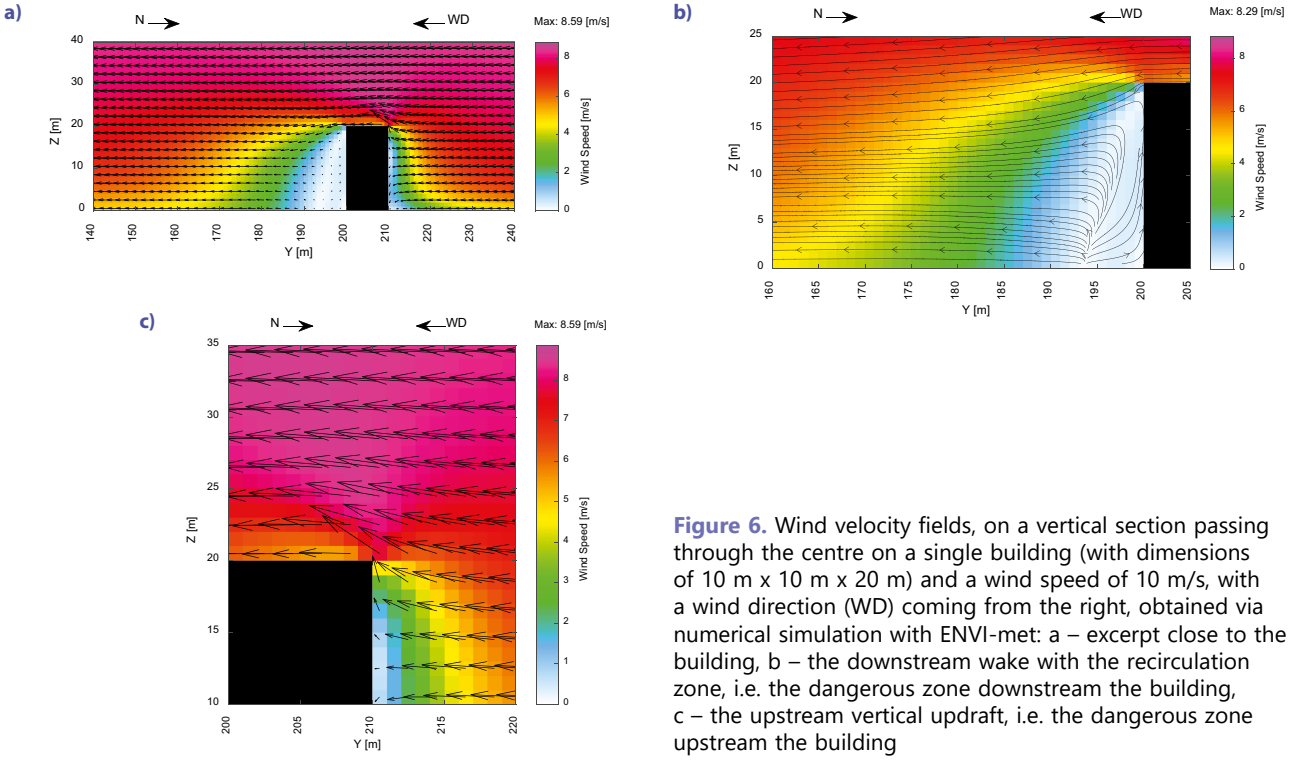

Figure 6. Wind velocity fields, on a vertical section passing through the centre on a single building (with dimensions of 10 m x 10 m x 20 m) and a wind speed of 10 m/s, with a wind direction (WD) coming from the right, obtained via numerical simulation with ENVI-met: a – excerpt close to the building, b – the downstream wake with the recirculation zone, i.e. the dangerous zone downstream the building, c – the upstream vertical updraft, i.e. the dangerous zone upstream the building

wind. The downstream wake distance, even if with some fluctuations, tends to increase when the building height and the wind speed increase. The downstream wake zone, which can be defined as the whole zone downstream the building inside the downstream wake distance, should be avoided for UAS operations.

The vertical updraft distance is measured in a vertical section of the velocity field at the building's midpoint. It is defined as the distance between the upstream upper corner of the building and the point where the velocity vectors become again horizontal. The vertical updraft distance has been measured for each simulated case and its values are shown in Figure 8, versus the building height, for each wind. Similarly, to the downstream wake distance, the vertical updraft distance tends to increase when the building height and the wind speed increase. The vertical updraft zone, which can be defined as the whole zone above the building rooftop inside the vertical updraft distance, should be avoided for UAS operations as well.

Figure 7 presents the relationship between building height (BH), wind speed (WS), and the extent of the downstream wake (DW) hazardous zone. This data was analysed to establish a mathematical relationship between these parameters. This analysis aimed to provide a practical equation for estimating the size of the dangerous zone for UAS operations, contingent upon wind velocity and building height.

An Equation (1) was empirically derived to estimate the downstream wake distance (DW) based on the simulation results. This formula recognizes DW as a function of both building height (BH) and wind speed (WS). The formula takes the form of a power-law relationship, incorporating two distinct components: a scale parameter and a shape parameter (DW = scale parameter * shape of parabola).

The DW scale parameter, represented by the expression $(k_{1DW} + k_{2DW} * (WS))$, accounts for the overall size of the downstream wake.

a) Constant Term, $k_{1DW} = 5.8$, which establishes a baseline wake length that persists even in minimal wind conditions. It reflects the inherent turbulence and flow disruption introduced by the building's presence.

b) Wind Speed Coefficient, $k_{2DW} = 0.19$, this coefficient modulates the wake length in response to variations in wind speed (WS). Stronger winds impart greater momentum and energy, causing the wake to elongate. The coefficient quantifies this effect, ensuring that the wake expands proportionally with increasing wind velocity.

The DW shape parameter, denoted by $BH^{1/3}$, dictates the geometric form of the wake, approximating it as a parabola.

Building Height Exponent signifies that the downstream wake length grows with the cube root of the building height (BH). Taller buildings generate larger, more pronounced wakes, and this exponent captures the non-linear growth observed in the simulation data.

The constants $k_{1DW} = 5.8$ and $k_{2DW} = 0.19$ were determined through an iterative optimization process, refining the formula to minimize the average prediction error across the entire dataset. The resulting Equation:

$$DW = (k_{1DW} + k_{2DW}\,(WS)) \cdot (BH)^{1/3} \quad (1)$$

achieves a high degree of accuracy, with deviations from the simulated data consistently below 5%.

Figure 7 provides a visual representation of the formula's implications. The five distinct curves illustrate the dependency between building height (ranging from 5 m to 20 m) and wind speed (ranging from 2 m/s to 10 m/s), showcasing how the wake length expands with both increasing building height and wind speed. The two dashed lines, representing the minimum (2 m/s) and maximum (10 m/s) wind speeds, effectively delineate the overall trend of wake length growth across the entire range of wind velocities, as predicted by the derived Equation (1).

Figure 8 illustrates the relationship between building height (BH), wind speed (WS), and the extent of the vertical updraft (VU) hazardous zone. This data, similar to the downstream wake analysis, was examined to establish a mathematical correlation between these parameters. The objective remained the same, to derive a practical equation for predicting the size of the dangerous zone for UAS operations, contingent upon wind velocity and building height.

The resulting Equation (2) for vertical updraft distance (VU) mirrors the structure of the downstream wake equation, adhering to the same power-law relationship and incorporating analogous scale and shape parameters.

The VU scale parameter, represented by the expression $(k_{1VU} + k_{2VU}*(WS))$, governs the overall magnitude of the vertical updraft.

a) Constant Term, $k_{1VU} = 1.06$, denotes the baseline updraft height, present even in calm conditions. It accounts for the inherent upward deflection of airflow caused by the building's facade.

b) Wind Speed Coefficient, $k_{2VU} = 0.2$, modulates the updraft height in response to variations in wind speed (WS). Stronger winds amplify the upward deflection, leading to a taller updraft. The coefficient quantifies this effect, ensuring that the updraft height increases proportionally with escalating wind velocity.

The VU shape parameter, expressed as $BH^{3/5}$, determines the geometric form of the updraft, approximating it as a parabola.

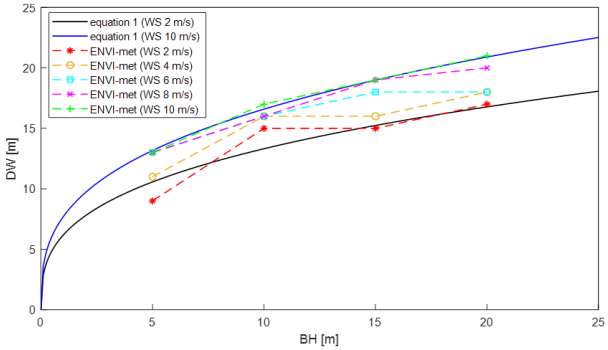

Figure 7. Graphical representation demonstrating the correlation between building height, wind velocity, and the extent of the hazardous zone – downstream wake zone

Building Height Exponent signifies that the vertical updraft height grows with the building height (BH) raised to the power of 3/5. This exponent, distinct from the 1/3 exponent in the downstream wake equation, reflects the steeper growth observed in the updraft data compared to the wake data. Taller buildings induce stronger updrafts, and the 3/5 exponent captures this accelerated growth rate.

The constants $k_{1VU} = 1.06$ and $k_{2VU} = 0.2$ were determined through an iterative optimization process, refining the formula to minimize the average prediction error across the dataset. The resulting Equation:

$$VU = (k_{1VU} + k_{2VU}(WS)) \cdot (BH)^{3/5} \quad (2)$$

achieves a high level of accuracy, with deviations from the simulated data generally within 6.1%

Figure 8 visually reinforces the formula's implications. The five distinct curves illustrate the dependency between building height (ranging from 5 m to 20 m) and wind speed (ranging from 2 m/s to 10 m/s), showcasing how the updraft height expands with both increasing building height and wind speed. Unlike the downstream wake, where the curves were relatively evenly spaced, the curves for the vertical updraft become more widely spaced as building height increases, reflecting the steeper growth rate captured by the 3/5 exponent.

4. AdMaS campus simulation

The second scenario examined a section of the AdMaS Centre at Brno University of Technology (Brno, Czech Republic) under typical spring/summer atmospheric conditions. This was done for two primary reasons:

1. to validate the information on the dangerous zones obtained from the stand-alone building simulations in a real-world scenario;
2. to develop a model that could be compared with real-time wind velocity data collected during UAS flights planned for the summer of 2024.

A detailed numerical simulation of the AdMaS research centre environment was conducted. This aimed to validate the formulas (Equations (1) and (2)) derived from the simplified single-building simulations in a real-world situation and to establish a baseline for future field experiments. This model serves a dual purpose:

a) Immediate validation: An assessment of the congruence between the sizes of the downstream wake and updraft distances was aimed for. These distances were measured around the main building (Building H) in the AdMaS complex using data obtained from numerical simulations. The measured values were compared to values calculated using the proposed empirical formulas. This comparison provides a preliminary assessment of the formulas' applicability to real-world configurations.

b) Future real-time data comparison: the model will serve as a virtual testbed for comparison with real-time wind velocity data collected during planned UAS flights in the summer of 2024. This comparative analysis will facilitate the further validation and refinement of the turbulence models, ensuring their robustness and applicability in informing safe and efficient UAS operations within complex urban environments.

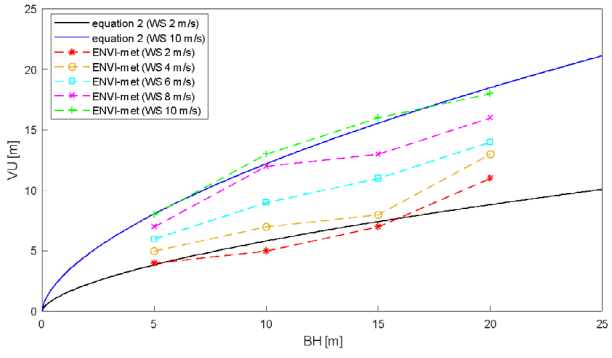

Figure 8. Graphical representation demonstrating the correlation between building height, wind velocity, and the extent of the hazardous zone – vertical updraft zone

Meteorological data acquisition and terrain characterization

To ensure the fidelity of the simulation, historical meteorological data for the AdMaS location was obtained from the "Meteomatics" service, a data provider whose reliability was previously validated in our prior research (Balážová et al., 2024). The data, spanning the spring/summer seasons of 2020–2023, corresponds to the anticipated timeframe of our field experiments.

The data, provided at 15-minute intervals, represented conditions at a specific location within the AdMaS research center, where a portable weather station would be installed during the 2024 summer demonstration mission.

Wind data, specifically wind direction and speed, were statistically analyzed and summarized using wind rose diagrams (Figure 9). This analysis revealed the predominant wind patterns in the AdMaS research center area.

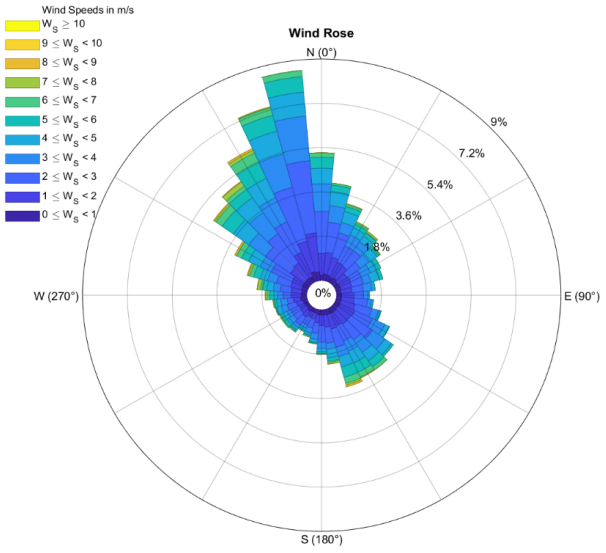

Figure 9. Wind rose of all spring-summer season (2020–2023)

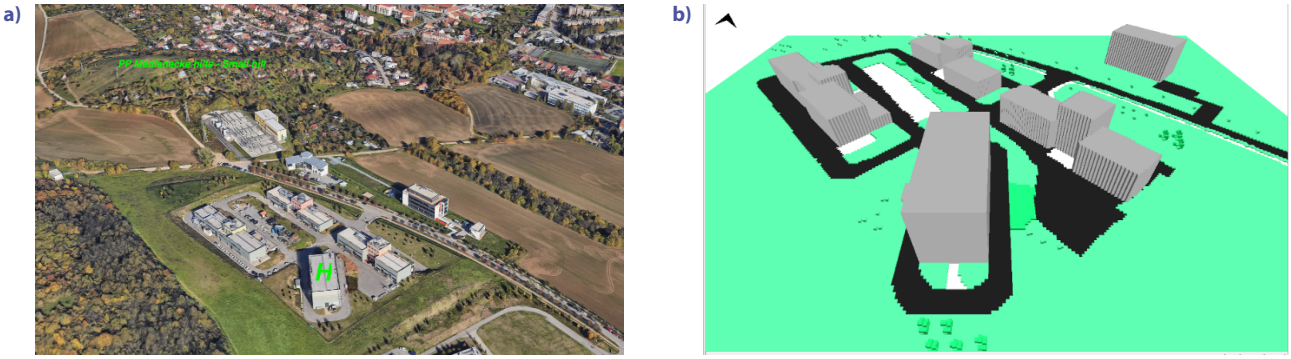

Figure 10. Domain for the real-world scenario simulations: a – map of AdMaS center (source: Google maps), b – a visualization of the related 3d simulated domain

Figure 9 presents a wind rose diagram, where the colours represent wind velocity, the bar position indicates wind direction, and the bar length represents the percentage of time the wind blew from that direction during the investigated period. Analysis of this figure shows that the most frequent wind directions were between 330–359 degrees, with the most frequent velocities ranging from 1 to 6 m/s. This information was used during design of simulation scenarios, ensuring that data reflected the most common wind conditions experienced at the AdMaS research center. As the 1 m/s velocity is considered not to be dangerous for the UAS operations, the simulations of the AdMaS center were performed with undisturbed velocities of 2, 4 and 6 m/s. The demonstration flights will be performed when the wind conditions will be within this simulated velocity range.

Topographical analysis of the surrounding terrain, particularly a prominent hill situated north of the AdMaS center, was conducted to build the simulation domain. Calculations of the reattachment distance (135–190 m), based on prevailing wind conditions and hill geometry (hill distance 450 m), indicated that the hill's influence (see the left panel of Figure 10) on airflow within the campus would be negligible. Consequently, and considering that the terrain is flat inside the AdMaS center, we delineated the simulation domain shown on the right panel of Figure 10. The domain was rotated to be aligned with the building H, around which the demonstration flights will be performed. Moreover, the modeling of buildings (materials and sizes), vegetation, and other pertinent features (e.g., pavements and roads) within the campus was done in the numerical model.

Formula validation and assessment

Wind flow patterns around Building H were simulated in ENVI-met under the predominant wind conditions identified through meteorological analysis. Figure 11 shows an example of the wind velocity field in a horizontal plane near the terrain level at 12:00, with an undisturbed wind speed of 4 m/s. Due to the above-mentioned rotation of the domain, in the Figure the wind comes from above. The downstream wake zones behind the buildings are visible.

In Figure 12, the wind velocity field in a vertical plane taken in the middle of the building H width at 12:00 p.m., with an undisturbed wind velocity of 4 m/s, is shown. In this Figure, the wind comes from the right and the interaction between the flow patterns between the buildings is visible; the building H is identifiable as the largest one on the left. This section was used to measure the dimensions

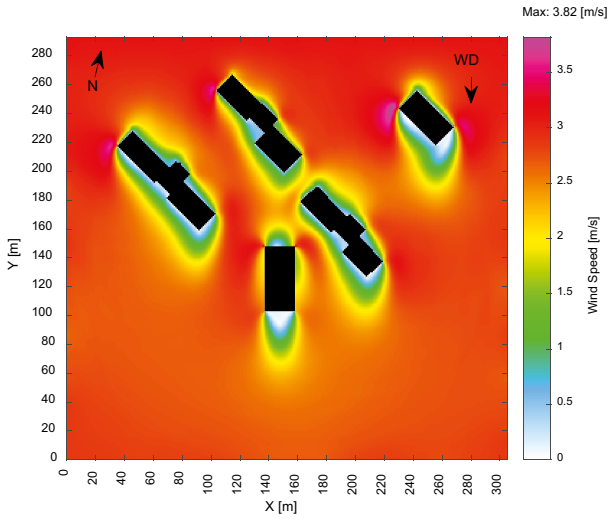

Figure 11. Wind velocity field in a horizontal plane close to the terrain level (9,5 m above the ground) at 12:00, extracted as an output of the ENVI-met numerical simulation of AdMaS centre with starting wind speed 4 m/s; wind comes from above

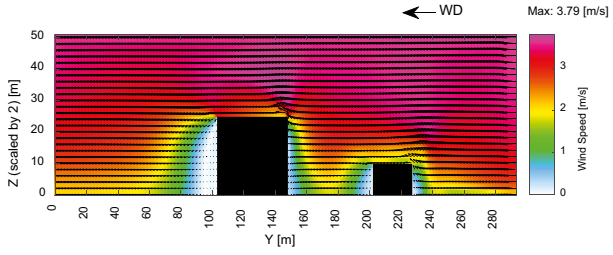

Figure 12. Wind velocity field in a vertical plane taken in the middle of the building H width at 12:00, extracted as an output of the ENVI-met numerical simulation of AdMaS centre with starting wind speed 4 m/s; wind comes from the right

Table 3. Comparison of calculated (via Equations (1) and (2)) and measured (on the numerical simulations of the AdMaS center) danger zone sizes

Building height [m]	Wind Speed [m/s]	Calculated wake distance [m] (Equation (1))	Measured dimension of DW distance [m]	Calculated vertical updraft distance [m] (Equation (2))	Measured dimension of VU zone [m]
25	2	18	19	10	10
25	4	20	20	13	15
25	6	21	21	21	18

of the downstream wake zone and the updraft zone. These zones were induced by the interaction between the wind flow and Building H in the presence of other buildings. The methodology used was the same as that illustrated in Section 3.1. In Table 3 these values were subsequently compared with the predicted sizes calculated using the empirical formulas derived from the single-building simulations (Equation (1) and Equation (2)).

The data presented in Table 3 compares the results of the AdMaS simulations (for building H with BH = 25 m) with the calculated values obtained using the refined equations 1 and 2. The formula for downstream wake distance (Equation (1)), demonstrates a good agreement with the simulation results. For wind speeds of 2, 4 and 6 m/s, the calculated wake distances of 18 m, 20 m, and 21 m, respectively, closely match the simulated values of 19 m, 20 m, and 21 m. These results indicate that the equation effectively captures the relationship between building height, wind speed, and downstream wake length for this specific building configuration. The formula for vertical updraft distance (Equation (2)), shows a generally good agreement with the simulation results for wind speeds of 2 m/s and 6 m/s. The calculated VU distances of 10 m and 21 m are very close to the simulated values of 10 m and 18 m, respectively. However, at a wind speed of 4 m/s, the calculated VU distance of 13 m slightly underestimates the simulated value of 15 m. This discrepancy can likely be attributed to the complex interaction between the incoming wind profile, the upstream buildings, and the specific shape of building H. The simplified model used in the formula might not fully capture these intricate interactions, leading to some deviation from the simulation results. In summary, the preliminary analysis indicates a favorable overall agreement between the simulated and predicted values for both the downstream wake and vertical updraft distances. This provides initial support for the applicability of the formulas to real-world building configurations. The discrepancies observed in the vertical updraft distance for a wind speed of 4 m/s highlight the importance of considering the complex interactions between buildings, terrain, and vegetation in determining the precise size of the dangerous zones for UAS operations in the built environment. While the current formulas offer valuable insights and predictions, future research could focus on refining the vertical updraft model to better account for these complex interactions and further reduce prediction errors. This could involve incorporating additional parameters, exploring alternative functional forms, or utilizing more sophisticated simulation techniques.

It is important to acknowledge that the simplified formulas presented in Equations (1) and (2) provide an estimation of the dangerous zones for UAS flights near buildings, but they may not perfectly predict the exact values in every situation. The real world presents a multitude of variables, such as complex building shapes, surrounding terrain, and varying atmospheric conditions, that influence the precise extent of these zones. While incorporating every single real-world variable into the model would lead to more complex formulas, it could also limit their practical applicability. The focus of this study is to provide a first-order approximation of the hazardous zones, offering UAS operators a practical tool for assessing risk and enhancing safety. The generally good agreement between the calculated and measured values, as seen in Table 3, supports the validity of this approach.

5. Conclusions

In this study, a multifaced approach to gain an advancement towards the operational estimation of EDR utilizing UASs and of dangerous zone size for the UAV flight at low altitudes and in presence of buildings was proposed. This multi-faceted approach, integrating sensor validation, numerical modelling, and preliminary real-world validation, contributes to a comprehensive understanding of low-altitude turbulence and its implications for UAS operations.

The first task of this work was the identification and test of a low-cost, low-weight sensor to measure the wind velocity on board an UAV, and then to validate its measurements through a comparison between in-field measurements, performed under real-world conditions, and laboratory measurements, performed under controlled and repeatable conditions. The successful validation of the Calypso "Ultrasonic Portable Mini" anemometer, coupled with the refined Eddy Dissipation Rate (EDR) calculation methodology, demonstrates its efficacy for in-situ turbulence assessment on UAV platforms.

The second task was the investigation of the size of the dangerous zones for the UAV maneuvers, via numerical simulations on the interaction of wind (with various velocities) and a single building (of various heights), using the data to propose some empirical formulas for predicting the extent of hazardous zones, such as downstream

wake areas and building edge updrafts, that are used to evaluate them. The empirically derived formulas for estimating downstream wake distances and building edge updrafts provide actionable safety guidelines, empowering UAS operators with critical information for risk mitigation. It is important to note that the presented data and formulas focus on the mean size of the dangerous zones for UAS flights near buildings. While turbulence fluctuations are inherently present in these zones, the models and equations presented here primarily capture the mean flow characteristics. This simplification is justified by the need to provide a practical and accessible tool for UAS operators. To account for the inherent variability of turbulence, a safety coefficient should be introduced when using the formulas to estimate the extent of the hazardous zones. This safety coefficient would provide a buffer zone, increasing the estimated size of the dangerous zones to account for potential fluctuations in wind speed and direction. Further research could explore the incorporation of turbulence fluctuations into the models to provide more refined predictions of the hazardous zones. These zones are characterized by distinct flow disturbances induced by the interaction of wind with buildings. For instance, the downstream wake zone exhibits low wind speeds and shifting wind directions due to wake vortices, while the vertical updraft zone above the building rooftop can cause undesirable lift. Understanding these flow disturbances is crucial for safe UAS operations near buildings.

The third task of this paper was the preliminary validation of the proposed formulas on a more complex real-world built environment. Through numerical simulation of the AdMaS research center under typical spring conditions: this preliminary validation underscores their potential applicability to real-world scenarios. However, further validation is necessary to ensure their robustness across diverse environmental conditions and building configurations.

Moreover, the upcoming demonstration mission at the AdMaS research center will serve as a pivotal step in this validation process. By collecting real-time turbulence data from UAS flights and juxtaposing it with the simulated results, turbulence models and developing a real-time turbulence warning system were refined as significant aim. This system will leverage the validated Calypso anemometer and refined EDR calculations to provide UAS operators with immediate, actionable alerts regarding potential turbulence hazards.

The AdMaS simulation model, calibrated with historical meteorological data and detailed terrain analysis, will function as a virtual testbed for this demonstration mission. The comparison of real-time data with simulated results will not only validate these existing models but also facilitate their refinement, leading to more accurate predictions and enhanced safety guidelines.

Beyond the immediate validation goals, this research lays the groundwork for a broader initiative to enhance the safety and operational efficiency of UASs within complex urban environments. Future investigations will focus on expanding field experiments to diverse urban settings, incorporating additional meteorological sensors for comprehensive data acquisition, and integrating our findings into actionable tools and decision support systems for UAS operators.

By addressing the critical gap in meteorological information for UASs operating at low altitudes, this research has the potential to significantly improve the safety, reliability, and overall capabilities of UASs in various applications, while also fostering their seamless integration into the complex airspace of the future.

Funding

This work was supported by the project No. FSI-S-23-8163 funded by the Ministry of Education, Youth and Sport (MEYS, MŠMT in Czech) institutional support, and by the project VJ02010036 (An Artificial Intelligence-Controlled Robotic System for Intelligence and Reconnaissance Operations) funded by the Ministry of the Interior of the Czech Republic (MVCR). The study was further supported by the infrastructure of RICAIP that has received funding from the European Union's Horizon 2020 research and innovation programme under grant agreement No 857306 and from Ministry of Education, Youth and Sports under OP RDE grant agreement No CZ.02.1.01/0.0/0.0/17_043/0010085. This work was partially supported by the University of Cagliari (Italy).

Author contributions

RB: study conceptualization; RB: methodology; RB, SF, AS: numerical simulation preparation and execution; RB, JH: sensor selection; RB: ground instrumentation preparation; RB, PG: UAS preparation and sensor integration; PG: UAS operation; RB, PG: field data collection; RB: data processing, evaluation and interpretation; RB: writing – original draft; RB, JH, PG, SF, AS: writing – review and editing.

Disclosure statement

The authors declare that there are no competing financial, professional, or personal interests from other parties related to this research work.

References

Adkins, K. A. (2019). Urban flow and small unmanned aerial system operations in the built environment. *International Journal of Aviation, Aeronautics, and Aerospace*, *6*(1). https://doi.org/10.15394/ijaaa.2019.1312

Adkins, K. A., Swinford, Ch. J., Wambolt, P. D., & Bease, G. (2020). Development of a sensor suite for atmospheric boundary layer measurement with a small multirotor unmanned aerial system. *International Journal of Aviation, Aeronautics, and Aerospace*, *7*(1). https://doi.org/10.15394/ijaaa.2020.1433

Balážová, R., Ferrari, S., Hlinka, J., & Santus, A. (2024) Turbulence estimation by Eddy dissipation rate at low-altitudes using UAV in-situ data. *Engineering Mechanics*, *30*, 42–45. https://doi.org/10.21495/em2024-042

Bruse, M., & Fleer, H. (1998). Simulating surface–plant–air interactions inside urban environments with a three dimensional numerical model. *Environmental Modelling & Software*, *13*(3–4), 373–384. https://doi.org/10.1016/S1364-8152(98)00042-5

Chiri, G. M., Achenza, M., Canì, A., Neves, L., Tendas, L., & Ferrari, S. (2020). The microclimate design process in current African development: The UEM Campus in Maputo, Mozambique. *Energies*, *13*(9), Article 2316. https://doi.org/10.3390/en13092316

Chrit, M. (2023). Reconstructing urban wind flows for urban air mobility using reduced-order data assimilation. *Theoretical and Applied Mechanics Letters*, *13*(4), Article 100451. https://doi.org/10.1016/j.taml.2023.100451

Chrit, M., & Majdi, M. (2022). Improving wind speed forecasting for urban air mobility using coupled simulations. *Advances in Meteorology*. https://doi.org/10.1155/2022/2629432

Diop, M., Dubois, P., Toubin, H., Planckaert, L., Le Roy J.-F., & Garnier, E. (2022). Reconstruction of flow around a high-rise building from wake measurements using Machine Learning techniques. *Journal of Wind Engineering and Industrial Aerodynamics*, *230*, Article 105149. https://doi.org/10.1016/j.jweia.2022.105149

ENVI-met. (n.d.). *Homepage*. http://www.envi-met.com

Ezaki, T., Fujitsuka, K., Imura, N., & Nishinari, K. (2024). Drone-based vertical delivery system for high-rise buildings: Multiple drones vs. a single elevator. *Communications in Transportation Research*, *4*, Article 100130. https://doi.org/10.1016/j.commtr.2024.100130

Fabbri, K., & Costanzo, V. (2020). Drone-assisted infrared thermography for calibration of outdoor microclimate simulation models. *Sustainable Cities and Society*, *52*, Article 101855. https://doi.org/10.1016/j.scs.2019.101855

Ferrari, S., Rossi, R., & Di Bernardino, A. (2022). A review of laboratory and numerical techniques to simulate turbulent flows. *Energies*, *15*(20), Article 7580. https://doi.org/10.3390/en15207580

Frey, J., Rienecker, H., Schubert, S., Hildebrand, V., & Pfifer, H. (2024). Wind tunnel measurement of the urban wind field for flight path planning of unmanned aerial vehicles. In *AIAA SciTech Forum and Exposition*. Aerospace Research Central. https://doi.org/10.2514/6.2024-2510

Galway, D., Etele, J., & Fusina, G. (2011). Modeling of urban wind field effects on unmanned rotorcraft flight. *Journal of Aircraft*, *48*(5), 1613–1620. https://doi.org/10.2514/1.C031325

Galway, D., Etele, J., & Fusina, G. (2012). Surveillance applications of unmanned aerial vehicles (UAVs) within urban areas is made difficult by turbulent winds generated by buildings. *Journal of Wind Engineering and Industrial Aerodynamics*, *103*, 73–85. https://doi.org/10.1016/j.jweia.2012.02.010

Giersch, S., Guernaoui, O. E., Raasch, S., Sauer, M., & Palomar, M. (2022). Atmospheric flow simulation strategies to assess turbulent wind conditions for safe drone operations in urban environments. *Journal of Wind Engineering and Industrial Aerodynamics*, *229*, Article 105136. https://doi.org/10.1016/j.jweia.2022.105136

Google. (n.d.). [AdMaS center].

International Civil Aviation Organization. (2001). *Meteorological service for international air navigation* (Annex 3 to the Convention on International Civil Aviation) (14th ed.). ICAO.

Kim, J., Kim, J.-H., & Sharman, R. D. (2021). Characteristics of energy dissipation rate observed from the high-frequency sonic anemometer at Boseong, South Korea. *Atmosphere*, *12*(7), Article 837. https://doi.org/10.3390/atmos12070837

Kristiansson, M., Andersson Hagiwara, M., Svensson, L., Schierbeck, S., Nord, A., Hollenberg, J., Ringh, M., Nordberg, P., Andersson Segerfelt, P., Jonsson, M., Olsson, J., & Claesson, A. (2024). Drones can be used to provide dispatch centres with on-site photos before arrival of EMS in time critical incidents. *Resuscitation*, *202*, Article 110312. https://doi.org/10.1016/j.resuscitation.2024.110312

Mellor, G. L., & Yamada, T. (1975). A simulation of the Wangara atmospheric boundary layer data. *Journal of the Atmospheric Sciences*, *32*(12), 2309–2329. https://doi.org/10.1175/1520-0469(1975)032<2309:ASOTWA>2.0.CO;2

Mohamed, A., Marino, M., Watkins, S., Jaworski, J., & Jones, A. (2023). Gusts encountered by flying vehicles in proximity to buildings. *Drones*, *7*(1), Article 22. https://doi.org/10.3390/drones7010022

Palomaki, R. T., Rose, N. T., van den Bossche, M., Sherman, T. J., & De Wekker, S. F. J. (2017). Wind estimation in the lower atmosphere using multirotor aircraft. *Journal of Atmospheric and Oceanic Technology*, *34*, 1183–1191. https://doi.org/10.1175/JTECH-D-16-0177.1

Patrikar, J., Moon, B. G., & Scherer, S. (2020). Wind and the city: Utilizing UAV-based in-situ measurements for estimating urban wind fields. In *2020 IEEE/RSJ International Conference on Intelligent Robots and Systems* (*IROS*). IEEE. https://doi.org/10.1109/IROS45743.2020.9340812

Pensado, E. A., Carrera, G. F., López, F. V., Jorge, H. G., & Ortega, E. M. (2024). Turbulence-aware UAV path planning in urban environments. In *2024 International Conference on Unmanned Aircraft Systems* (*ICUAS*) (pp. 280–285). IEEE. https://doi.org/10.1109/ICUAS60882.2024.10556934

Simon, H., Heusinger, J., Sinsel, T., Weber, S., & Bruse, M. (2021). Implementation of a Lagrangian stochastic particle trajectory model (LaStTraM) to simulate concentration and flux footprints using the microclimate model ENVI-Met. *Atmosphere*, *12*(8), Article 977. https://doi.org/10.3390/atmos12080977

Szucs, A. (2013). Wind comfort in a public urban space – case study within Dublin Docklands. *Frontiers of Architectural Research*, *2*(1), 50–66. https://doi.org/10.1016/j.foar.2012.12.002

Wang, Y. Z. D., & Lv, L. (2019). Comparative study of urban residential design and microclimate characteristics based on ENVI-met simulation. *Indoor and Built Environment*, *28*(9), 1200–1216. https://doi.org/10.1177/1420326X19860884

Yuan, W., Zhang, X., Poirel, D., & Wall, A. (2024). Numerical modelling of aerodynamic response to gusts and gust effect mitigation. *Aerospace Science and Technology*, *154*, Article 109467. https://doi.org/10.1016/j.ast.2024.109467